GROUND-BASED GAS-LIQUID FLOW RESEARCH IN MICROGRAVITY CONDITIONS:

STATE OF KNOWLEDGE

J. McQuillen

National Aeronautics and Space Administration, Lewis Research Center,

21000 Brookpark Road, Cleveland, OH 44135

C. Colin and J. Fabre

Institut de M'ecanique des Fluides de Toulouse, URA CNRS 005,

Avenue Camille, Soula, 31400 Toulouse, France

Send Correspondence to:
John McQuillen
NASA Lewis Research Center
MS 500/102
21000 Brookpark Road
Cleveland, OH 44135
PH: (216)433-2876
FAX: (216)433-8660
e-mail: j.mcquillen@lerc.nasa.gov

ABSTRACT

During the last decade, ground-based microgravity facilities have been utilized in order to obtain predictions for spacecraft system designers and further the fundamental understanding of two-phase flow. Although flow regime, pressure drop and heat transfer coefficient data has been obtained for straight tubes and a limited number of fittings, measurements of the void fraction, film thickness, wall shear stress, local velocity and void information are also required in order to develop general mechanistic models that can be utilized to ascertain the effects of fluid properties, tube geometry and acceleration levels. A review of this research is presented and includes both empirical data and mechanistic models of the flow behavior.

KEYWORDS:

Two-phase Flow, Microgravity, Flow Regimes, Heat Transfer Coefficients, Pressure Drop.

INTRODUCTION:

Gas-liquid, vapor-liquid flows exist in a wide variety of applications in both the normal gravity and reduced-gravity environments. As is usually the case, there are many benefits and drawbacks to the use of two-phase systems, and consequently serious considerations are needed before deciding on whether or not to proceed with the design, construction and use of these systems, particularly in a reduced-gravity environment. In some circumstances

though, there is no luxury of a choice between single- or two-phase system, the circumstances will dictate that some form of a two-phase system must be accommodated.

In normal gravity, or terrestrial, applications, gas-liquid flows have been traditionally studied by the petroleum and nuclear industries. The petroleum industry has focused most of their efforts on flow through long pipelines with the intent of transferring a mixture of crude oil and natural gas from the well and then performing the separation of the components and/or products at the refinery. The nuclear industry has been concerned with system stability and safety with the primary intent of preventing dryout of the nuclear reactor through either a heat transfer/fluid flow instability or loss of coolant accident as the heat energy is transferred from the reactor to the turbines driving the electric generators. The chemical industries have utilized gas-liquid contacters to increase interfacial mass and heat transfer in absorption, stripping and distillation processes that involve two-phase flows through complex geometries.

In a reduced-gravity environment, the terminology becomes much more grandiose, as can be seen in Swanson *et al.*(1989)[1], although the principles remain the same,. Power generation involves the transfer of heat from the source to an electrical generator. For the most part, several systems in Earth orbit rely on photovoltaic systems; however, there have been studies that indicate that for a power system requiring more than 25 kW, a solar dynamic Rankine cycle is much more efficient in terms of the launch mass of the system and the propellant required to overcome any drag encountered on the devices used to collect the

solar energy. Two-phase systems also offer the capability of isothermally temperature control.

Thermal management systems are quite often coupled, figuratively and literally, with power management systems, although, power management systems deal with the transfer of heat energy to perform useful work whereas thermal management systems transfer waste heat from a source to a sink, typically through a radiator panel. The sources for waste heat include thermodynamic heat rejection for power generation cycles, resistance heat from electronic equipment and power management and distribution systems, and exothermic biological activity.

For both power and thermal management systems, alternatives to two-phase systems exist. For example, during the development of the space station power systems, photovoltaics and a single-phase gas Brayton cycle were evaluated, and received higher preference than the Rankine two-phase system. Single-phase systems are also used for the thermal management systems. Such decisions are often based on risk mitigation associated with the more predictable behavior of single-phase systems in reduced-gravity.

Fluid management is the transfer of fluids from one tank to another and also involves acquiring the fluid from the tank to the transfer line and metering the amount of fluid transferred. Cryogenic liquids are typically required for use as propellants and to cool certain types of equipment and sensors; however, transferring the liquid generates vapor as the

liquid contacts the warm surfaces, such as the transfer lines and receiving tanks. Depending on the characteristics of the supply tank, that is if it is not a variable volume container such as a bladder or bellows type accumulator, the transfer of "storable" liquids, such as water, can result in a two-phase flow as the pressurizing gas enters the transfer line with the liquid.

Environmental Control and Life Support Systems (ECLSS) are responsible for maintaining temperature and humidity levels in manned spacecraft within comfortable levels given that biological activity is exothermic and increases the water vapor content within the atmosphere.

As with the designers of terrestrial systems, designers of space-based gas-liquid systems attempt to address two key issues: Will the system work and how reliable is the system? As such, they focus on predictions for the pressure drop in order to size pumps, the heat transfer coefficient for the design of heat exchangers, and the system stability as a means of accident prevention. However, as will be discussed, in order to make predictions based on one type of fluid system and tube geometry, additional measurements are required in order to develop fundamental models.

BENEFITS OF UTILIZATION OF GROUND-BASED FACILITIES

In order to design space-based systems, engineers require an understanding of the effect of gravity (or in this case, the lack thereof) on the behavior of the two-phases as they flow

through the system. The timely gathering of long-term microgravity data is primarily inhibited by the relative lack of opportunities to conduct space-based experimentation. The development of space-based experiments usually are expensive, have long lead-times from concept until the actual space-flight.

Fortunately, alternative methods of gathering low gravity data are available and have been utilized through the years. Aircraft, and, to a lesser extent drop towers, have been used to gather gas-liquid data. These facilities enable a significantly less time to design, build and test experiments than space experiments. In addition, the experimental hardware tends to be easier to modify and changes in the test matrix can be quickly accommodated.

Aircraft-based facilities provide longer, but poorer quality, periods of reduced-gravity than drop towers. However, this is not only reason that the aircraft facilities are preferentially used. Because of the flow development for the two-phase flow pattern, the ability to have long straight lengths of tubing is necessary. Typically, the flow pattern is considered to be fully-developed at a location of at least 100 length to diameter's (L/D) from its point of origin. Consequently, the longer the length of straight tubing, the larger the tube diameter at fully-developed flow conditions that can be tested. Drop tower packages are typically limited from 1 to 1.5 m in any dimension. The size of the drop tower package also restricts the amount of fluids that can be carried aboard the package.

Besides better quality periods of low gravity, however, drop towers do offer one other advantage over aircraft. That is the ability to establish a flow condition in normal gravity and then step-change into a period of microgravity to assess any residual effects from momentum and natural convection on the flow. Aircraft typically experience a period of high gravity (about 2 g's) and transition into low gravity over a period of 2 to 4 seconds.

DESCRIPTION OF GAS-LIQUID FLOWS IN NORMAL GRAVITY

Many studies have documented the effect of gravity on the flow behavior which can be easily seen in Figures 1 and 2.

Figures 1 & 2:

There are four basic flow regimes that have been identified for vertical flow in a normal gravity environment: Bubbly, slug, churn and annular.

- Bubbly flow consists of small gas bubbles suspended within a continuous liquid phase.

- Slug flow consists of long cylindrical-shaped bubbles with a spherical nose (usually referred to as a Taylor bubble) surrounded peripherally by a thin liquid film and

separated by liquid slugs. The liquid slugs and thin liquid film may or may not contain smaller gas bubbles.

- Churn flow is a more frothy and disordered form of slug flow except that the Taylor bubble is much more narrow and its shape is distorted. The continuity of the liquid phase within the slug between successive Taylor bubbles is repeatedly penetrated by a high local gas phase concentration. As the slug is penetrated, it falls, gathers additional liquid from the liquid film around the Taylor bubble, and re-bridges the diameter of the test section. After the slug has reformed across the diameter, it climbs until it is penetrated again. This falling and rising of the slug is the "churning." The existence of a "churn" flow regime is subject to much debate over its existence as to whether it is really a distinct flow regime or is just a transitional flow condition for slug flow.

- The annular flow regime consists of a thin liquid film on the wall that surrounds a gas core. Waves of liquid are transported across the thin liquid film and generate liquid droplets which are suspended within the gas core and then eventually deposited back into the liquid film

In horizontal flow, a stratified flow regime exists at relatively low flowrates whereby the two-phases are separated based upon their density difference. Slightly higher gas flowrates will start the formation of waves on the otherwise tranquil liquid surface. In this orientation, bubble, slug (called plug) and annular flow also exist; however, the flow pattern is non-

axisymmetric with very thin liquid films along the top of the tube and much thicker films along the bottom.

Gravity induces density-driven shear forces that affects the behavior of the flow and the phenomena being observed. For bubbly flow, shear forces based on the density difference between the phases opposes bubble coalescence. For slug and annular flow, the liquid film in normal gravity vertical up-flow will reverse its direction, rising with passage of a liquid slug or roll wave and then slowing, stopping and falling between slugs or waves. The liquid near the wall is carried up from the shear imparted by the slug or roll wave; however, the gas phase shear is insufficient to support, let alone carry the liquid adjacent to the wall.

As such, it has been determined that the influence of gravity on gas-liquid flows is demonstrated by simply changing the orientation of the flow direction with respect to gravity. Changes in the flow regime, as well as the liquid film thickness and void fraction, have been documented by changing the angle between the gravity vector and the flow direction for as little as 0.25^{o}[2]. There are also changes in the pressure drop which is attributable to changes in the hydrostatic head as the angle between the gravity vector and the flow direction are changed.

BRIEF HISTORICAL ACCOUNT OF PRIOR LOW GRAVITY RESEARCH:

In order to facilitate the development of "advanced" concepts for space power systems, several studies were undertaken to ascertain the effect of microgravity on the behavior in the 1960's. Evans (1963)[3], who was concerned with the design of heat exchangers, examined the effect of spiral inserts on bubble and slug flow in 12.7 mm inner diameter tube for both reduced and normal gravity. Evans determined that the liquid phase would be adjacent to the wall which is of practical concern to those designing heat exchangers. Albers and Macosco (1965)[4] measured the pressure drop for a condensing mercury vapor flow in reduced-gravity, thus providing the first quantitative data and found negligible difference for the pressure drop between normal gravity and reduced-gravity .

Heppner, King and Littles (1975)[5] and (1978)[6] conducted extensive testing aboard the KC-135 in a 25.4 mm inner diameter tube using air and water as part of reduced-gravity technology development. They obtained slug and annular flow, but flowrate limitations prevented them from obtaining bubble flow. They used high speed photography to recorded the flow regime and also measured the pressure drop. Unfortunately, since the test section only had a length to diameter ratio of 20, and most of their data was classified as "entrance effects." They attributed the flow pattern to the mixer design, but did not test alternative mixer configurations.

Several studies on two-phase flow, with or without phase change, have been carried out over the past ten years in order to understand the role of the gravity on the flow behavior,

focusing primarily on the description of the flow patterns and the prediction of the transitions between flow patterns. Some results on pressure drop, heat transfer coefficients and mean void fraction have been published, and, more recently, local measurements have been performed and examinations of conduit geometry have been undertaken.

REDUCED-GRAVITY FLOW REGIMES AND TRANSITIONS:

The classification of two-phase flow by various patterns, although subjective, is easy to accomplish since it only requires a careful observation of pictures taken with high-speed film or video camera. Different studies have been performed with various fluids, in tubes of different diameters, D, and different lengths, L, during reduced-gravity periods of about 20 s during aircraft parabolic trajectories, or 2.2 s in the NASA Lewis Research Center's Drop Tower. The fluids used were either air and water, or boiling Refrigerant 12 or 114. Different flow pattern have been identified at different superficial velocities of liquid, j_L, and gas, j_G.

Three flow patterns, Figure 3, have been observed in microgravity conditions. Two of them, bubbly and annular flows are called simple flow patterns because they are spatially homogeneous. The third pattern, called slug flow, is an intermediate flow pattern resulting from a transition of bubbly flow or annular flow and is spatially non-homogeneous. A fundamental question is what mechanisms are responsible for the transition between the spatially homogeneous flow patterns and the non-homogeneous pattern.

Figure 3

At low void fraction, bubbly flow occurs. At high superficial liquid velocity and low superficial gas velocity, small bubbles, a few millimeters in diameter, appear and are nearly spherical. Their motion is rectilinear with nearly the same velocity. The fluctuating motion is weak, contrary to what is observed in normal gravity up-flow where bubbles of ellipsoidal shape rise with a fluctuating motion. The size of the bubbles is mainly controlled by coalescence as suggested by the evolution of the size distribution between the inlet and the outlet of the pipe, Colin *et al.* (1991) [7]. As the void fraction increases, larger bubbles are created that move along the tube axis. When their size is comparable to the tube diameter, they take an oblate shape which is limited by the tube size. Following the classification proposed by Dukler *et al.*(1988)[8], the transition from bubbly to slug flow is defined when some bubbles with diameter larger than 1D or 2D appear. However, this transition is somewhat arbitrary since the larger bubbles grow with an increase in void fraction. There is no physical evidence of a pattern "bifurcation" (Colin *et al.*, 1991).

These large bubbles are the precursors of cylindrical bubbles that appear in slug flow at higher void fractions. These long bubbles which have a smooth interface and a spherical shaped nose, are separated by liquid slugs. These slugs contain smaller spherical bubbles moving nearly at the same velocity than the cylindrical bubbles. In contrast to normal gravity up-flow, these bubbles are not created by gas entrainment at the rear of the cylindrical

bubbles, but are simply the residue of the initial bubbly flow which is injected at the inlet and coalesced into larger bubbles as they proceeded downstream.

As additional gas is introduced, the liquid slugs decrease in length, and when the slugs become short enough, they collapse. At this point, the liquid slugs have massive gas bubble entrainment, are occasionally penetrated by the gas phase, and this condition is known as frothy slug-annular flow (Zhao and Rezkallah, 1993[9]). This flow pattern is a transitional regime between slug flow and annular flow since it contains elements of both flow regimes.

Annular flow consists of liquid flowing in the form of a thin film on the wall and gas flowing in the center and occurs at the highest superficial velocities of the gas. Liquid droplets are entrained in the gas core and are sheared off from waves traversing along the liquid film.

Reinarts (1993) and Bousman (1995) obtained data for flow behavior not only at acceleration levels less than ± 0.01g's, but also at lunar gravity, 0.17 g's and Martian gravity, 0.33 g's.

Transition Between Bubble and Slug Flow

Several authors have tried to predict the transition between bubble and slug flows using the arbitrary criterion that the transition will occur as the bubble diameter reaches a size equal to the tube diameter, but the most accepted approach was used by Dukler *et al.* (1988) and

Colin *et al.* (1991). The basis for the transition from bubbly to slug flow is the coalescence between bubbles and the rate of coalescence is dependent on the number of collisions which is a function of the bubble packing. Dukler *et al.* (1988) showed that the void fraction of mono-dispersed bubbles at maximum packing cannot exceed 0.53. They found that the transition occurs at a critical void fraction α_c of about 0.45. Colin *et al.* (1991) used a drift-flux relationship to determine the gas velocity, U_G, with respect to the mixture:

$$U_G = C_0(j_G + j_L) \tag{1}$$

where j_G is the superficial gas velocity and j_L is the superficial liquid velocity. An experimental value of 1.2 was found for C_0 in bubbly and slug flow. With the use of Equation 1, the transition may be expressed as:

$$j_L = j_G \frac{1 - C_0\alpha_c}{C_0\alpha_c} \tag{2}$$

For air and water flow experiments in tube with inside diameter smaller than 20 mm (Colin and Fabre, 1995[10] ; Dukler *et al.*, 1988; Huckerby and Rezkallah, 1992[11]; Bousman and Dukler, 1993[12]), the transition occurs for a critical value of the void fraction α_c equal to 0.45. In contrast, for air-water flow in 40 mm (Colin *et al.*, 1991) and in 25.4 mm (Bousman, 1995[13]) diameter tubes, and for R12 flows in 10.5 mm tubes (Reinarts, 1993), the transition takes place for a critical void fraction smaller than 0.2.

Colin *et al.* (1996)[14] assembled these data in and found that the transitional void fraction is a function of the pipe diameter D, the liquid viscosity ν_L, the liquid density ρ_L and the surface tension σ:

$$N_D = \frac{Re^2}{We} = \frac{\sigma D}{\rho_L v_L^2} < 1.5 \times 10^6 \rightarrow \alpha_C = 0.45,$$
$$N_D = \frac{Re^2}{We} = \frac{\sigma D}{\rho_L v_L^2} > 1.7 \times 10^6 \rightarrow \alpha_C = 0.20 \quad (3)$$

Equation 3 suggests a transition between the inhibiting–coalescence regime and the promoting–coalescence regime and that this transition is based upon the Suratman Number, $N_D = Su$, which is a function of the Reynolds Number, *Re*, and the Weber Number, *We*. The existence of such a transition criteria demonstrates that bubble coalescence plays a major role in microgravity. Although this correlation seems able to predict the transition from bubbly to slug flow, it does not provide any insight to the coalescence mechanism controlling this transition and does not account for the bubble size at the injection and the tube length.

Transition Between Slug and Annular Flow

Different authors have studied the transition from slug flow to annular flow including Dukler *et al.* (1988), Hill and Best (1991)[15], Huckerby and Rezkallah (1992), Bousman and McQuillen (1994)[16]. Based upon experimental results, there have been different approaches for the prediction of this transition.

For the transition from slug flow to annular flow, Dukler *et al.* (1988) assume that the void fraction, α, must be a continuous function of the flow rates, even at the transition since annular flow results from a continuous reduction of the liquid slug length. The transitional void fraction calculated from the models for both slug flow and annular flow must be equal.

The result found by equating the values of the void fraction calculated for slug flow, Equation (2), and the momentum balance for annular flow is

$$j_L = j_G \left[\frac{(1-\alpha)^2 \rho_G f_i}{\alpha^{2.4} \rho_L f_G} \left(\frac{\nu_G}{\nu_L} \right)^{02} \right]^{5/9} \tag{4}$$

where ν_G and ν_L are the kinematic viscosities of the gas and the liquid respectively, ρ_G and ρ_L are the densities of the gas and liquid respectiviely, f_i is the interfacial friction factor and f_G is the friction factor of the gas phase assuming that the liquid interface behaves like a smooth wall for the gas phase. Bousman and Dukler (1994), using Equations 3 and 2 and experimental values of f_i, found that the transition between slug flow and annular flow occurs at a critical void fraction of 0.755. The value of the critical void fraction is very sensitive to the modelling of f_i and care must be exercised when using models for f_i that were developed for normal gravity flow.

In a second approach, Reinarts (1993) suggests that the transition from slug flow to annular flow, is characterized by a Weber number of the gas phase. He assumed that for high enough velocity, the gas inertia is sufficient to break the bubble nose which is maintained by surface tension, σ. If r_p is the radius of the bubble nose, a crude force balance yields:

$$\frac{\rho_G U_G^2}{2} = \frac{2\sigma}{r_p} \tag{5}$$

By setting r_p equal to the radius of the air core in annular flow, $r_p = D\sqrt{\alpha}/2$, equation (5) becomes:

$$j_G = \left(\frac{8\sigma}{\rho_G D} \alpha^{2/3} \right)^{1/2} \tag{6}$$

Equation 6 together with Equation 4 relates the superficial velocities of the liquid and gas phases in order to determine the transition between slug and annular flow patterns. If the bubble nose is destabilized, it should result from the liquid motion which has the more effective inertia. As a result, the comparison with experimental results of other authors does not give credit to the theory (Colin and Fabre, 1995).

In a similar approach, based on the same physical considerations, Zhao and Rezkallah (1993) assumed that the transition between slug and annular occurs at a critical value of a Weber number:

$$We_{GS} = \frac{\rho_G j_G^2 D}{\sigma} \tag{7}$$

They observed the transition from slug to frothy slug-annular flow when We_{GS}=1 and the transition between frothy slug-annular and annular flows when We_{GS}=20. As a consequence the transitions should occur at a critical value of the superficial gas velocity, whatever the liquid velocity. This is not supported by the experiments of Bousman and McQuillen (1994) and Colin and Fabre (1995), which clearly show that at low superficial liquid velocities, the

transition from slug to frothy slug-annular flows and from frothy slug-annular to annular flows occur at a smaller gas velocity.

Jayawardena *et al.* [17] recently empirically applied a Suratman Number criteria to predict the transition between annular and slug flow:

$$Su = \frac{\sigma D}{\rho_L V_L^2} < 1\times 10^6 \rightarrow \frac{Re_{GS}}{Re_{LS}} = 4641.6\,Su^{-2/3}, \qquad Su = \frac{\sigma D}{\rho_L V_L^2} > 1\times 10^6 \rightarrow Re_{GS} = 2x10^{-9}\,Su^2 \tag{8}$$

The primary advantage of this technique is the data from an entire experiment set, tube diameter and fluid, will collapse into a single horizonal line (Su) when plotted with an independent variable of either Re_{GS} or Re_{GS}/Re_{LS}. However, this technique also sheds no light as to the transition mechanism.

Conclusions:

The transition from bubbly to slug flow appears to result from a progressive increase of the bubble size along pipe. There is no physical evidence of a pattern ''bifurcation'' as is the case in normal gravity up-flow. Until now, no mechanistic models were able to predict the bubble to slug transitions; however, one correlation based on the tube diameter and the fluid properties can be used to predict the bubble to slug transition will occur at a critical void fraction of 0.2 or 0.45. However, this is still only a correlation and it must be validated by other experiments. The coalescence between bubbles has been clearly identified as the

mechanism responsible for the transition, but the physics still are not understood. The influence of entrance conditions and of the pipe length on the flow development still need to be ascertained.

For the prediction of the transition from annular to slug flow, two mechanistic models, Dukler *et al.* (1988) and Reinarts (1993), and two correlations, Zhao and Rezkallah (1993) and Jayawardena *et al.* (1997), exist. The models require the use of the interfacial friction factor that is calculated based on data from normal gravity experiments. The critical void fraction at the transition predicted by the models is very sensitive to the value of the interfacial friction factor. It should be noted that there is no agreement between these the models and correlations. The physics are poorly understood. The transition between slug and annular flow is probably due to an liquid film instability, but this basic mechanism is not accounted for in the models.

PRESSURE DROP AND WALL FRICTION

In microgravity, the friction at the wall is directly related to the pressure drop, *dP/dx*. Indeed, the mean wall shear stress, τ_w, may be expressed as follows:

$$\tau_w = (\frac{D}{4})\frac{dP}{dx} \qquad (9)$$

Measuring the pressure drop is one method to determine the wall shear stress in bubbly and slug flow. This holds for normal gravity horizontal flow as well. Few results have been published for bubbly or slug flow. It was pointed out by Chen *et al.* (1991)[18] that in microgravity, the frictional pressure drops are generally greater than for normal gravity horizontal flow.

What controls the wall friction in bubbly flow? A current method to address this question uses an analysis of the friction factor, which is defined as follows:

$$f_p = \frac{2\tau_w}{\rho U^2} \tag{10}$$

Colin *et al.* (1996) showed that the correct scales for U and ρ are the liquid velocity and density. As the void is mainly concentrated along the tube axis, the momentum transfer at the wall is primarily governed by the liquid motion. This conclusion is supported by Figure 4 which proves that at the first approximation, the single-phase turbulent flow Blasius relationship works well for liquid Reynolds numbers between 20,000 and 80,000. The experimental data does not agree well for liquid Reynolds numbers less than 20,000. This proves that the presence of the second phase has some small influence upon the wall friction. Gas bubbles homogenize the liquid velocity in the radial direction. As the Reynolds number decreases, the thickness of the viscous layer increases, but the presence of large bubbles may affect this layer near the tube wall. This is due to an additional turbulence production induced by the distortion of the liquid flow vorticity by the bubble motion. This extra

turbulence was demonstrated for bubbly flow at microgravity conditions by Kamp *et al.* (1993).

Figure 4

Another interesting result which appears in Figure 4 concerns the transition between the laminar and turbulent regimes. For single-phase flow experiments that were carried out in 6 and 10 mm diameter tubes, the Reynolds numbers was between 1,000 and 40,000. In the 6 mm diameter tube, when the single-phase flow is laminar, the wall friction factor follows the theoretical Poiseuille relationship. The transition from laminar to turbulent flow is observed at Re_L » 8,000 for single-phase flow in the 10 mm diameter tube, with the jump at Re_L= 2100 typically being the signature of this transition. Clearly, two-phase bubbly flow does not display the same behavior at least for $Re_L > 4{,}000$.

There are some interesting and yet unresolved questions related to this: How does the wall friction behave at smaller Reynolds numbers? Does a laminar to turbulent flow transition exist and does the wall friction decrease?

Experimental results for slug flow are plotted in Figure 5. In comparison to bubbly flow, the same trends are observed, although the experimental data are much more scattered. The fundamental difference between bubbly and slug flow is the intermittence.

Figure 5

In a reference that moves with the long cylindrical bubbles, the flow appears almost frozen in microgravity. Indeed, each long bubble is separated by liquid slugs that contain small bubbles moving at about the same velocity as the long bubbles. By using the unit cell concept proposed by Wallis (1969)[19], the wall shear stress may be expressed in terms of the wall shear stress in the slug and of the wall shear stress in the long bubbles (Dukler and Fabre[20]):

$$\tau_W = \beta \tau_{WB} + (1 - \beta)\tau_{WS} \qquad (11)$$

where the subscripts B and S stand for the long bubble and slug regions respectively and β is the occurrence rate of the long bubbles as shown in Figure 6. In order for the wall shear stress to be written in this form, the flow must be fully-developed in both the long bubble and the slug regions. In the absence of gravity, there is no driving force to move the liquid film surrounding the long cylindrical bubbles. This is confirmed from the video sequences, because the liquid velocity can be estimated from the motion of tiny bubbles in the liquid film. Thus, the shear stress of the long bubbles is probably weak in comparison to that of the liquid slugs. Consequently, Equation 11 becomes

$$\tau_W = (1 - \beta)\tau_{WS} \qquad (12)$$

Figure 6

Using these assumptions, the shear stress for slug flow should be lower than that for bubbly flow. This is not supported by experimental results (Colin and Fabre 1995) which showed just the opposite. To arrive at this paradox, two assumptions were made: The flow in each region is fully-developed, and the friction in the liquid film is weak enough to be disregarded. It is likely that the second assumption is correct. However, since the slugs are short, the velocity profile can hardly be considered to be fully-developed in the moving reference. Thus, the first assumption needs to be reconsidered in order to predict the correct wall friction in slug flow.

Most of the results for pressure drop reported in the literature is for two-phase flow at high void fraction, i.e. in the annular or slug flow regimes. Zhao and Rezkallah (1993)[21] performed a curve fit on their annular flow data for an air-water system in a 9.5 mm diameter tube and found the two-phase multiplier, Φ^2_L, to take the following expression:

$$\Phi_L^2 = \frac{(dP/dx)_{TP}}{(dP/dx)_L} = 260x^{3/4} \qquad (13)$$

where x is the quality and the subscripts, TP and L refer to the two-phase and single-phase liquid pressure drop respectively.

Abdollahian *et al.* (1996)[22] found that the homogenous and Friedel models predicted satisfactorily the experimental data obtained in a 9.5 mm diameter tube with liquid and vapor R-114, while the results from using the Chisholm and Lockhart-Martinelli models were not as good. Unfortunately, no direct assessment of the flow regime by visualization was

possible and the assessment of the flow regime was based on the heater power and mass flow rate.

Zhao and Rezkallah, (1995)[23] compared data from all three flow regimes using the homogenous, Lockhart-Martinelli and Friedel models, and found that the Friedel model provided the best agreement with data obtained for air and water flowing in 9.5 mm diameter tube.

Bousman and Dukler (1994) determined empirically from data obtained for air with either, water, a 50% water and glycerine solution, or a 20 dyne/cm water and surfactant mixture, the following relationship for $0.75 < \langle\alpha\rangle < 0.85$:

$$\Phi = \frac{f_i}{f_G} = 2.114 - 245.9\langle\alpha\rangle \tag{14}$$

This model is of a similar form as the Wallis model (1969) that has been used for normal gravity flow as well as in microgravity, but there is a significant discrepancy between the Wallis model, Equation 15, and Equation 14.

$$\Phi = \frac{f_i}{f_G} = 1 + 150(1 - \langle\alpha\rangle^{1/2}) \tag{15}$$

In addition, as the void fraction approaches unity, f_i should approach f_G, but this is clearly does not occur for Equation 14 but does occur for the Wallis model. Obviously, this also has implications for the flow regime transition modeling, since Dukler *et al.* (1988) uses the Wallis model in the development of the transition from slug to annular flow.

Those these correlations can provide estimates for the pressure loss in annular flow, there has been very little work regarding the fundamental physics. Bousman and McQuillen (1994) suggested that the total pressure drop for annular flow in a microgravity environment was not of the form found in Equation 9, which works well for bubble and slug flow, but consists of two portions: That due to the wall shear, *W*, and that due to droplet entrainment, *E*, in the gas core:

$$\left(\frac{dP}{dx}\right)_{Total} = \left(\frac{dP}{dx}\right)_{W} + \left(\frac{dP}{dx}\right)_{E} \tag{16}$$

Furthermore, they found as the liquid film thickness would decrease, so would the wall shear stress. A comparison between data obtained for water and water with a surfactant revealed that while the total pressure drop was relatively unaffected, the liquid film thickness was much smaller, and thus the wall shear stress, for the water-surfactant mixture. They theorized that for this mixture, droplet entrainment was responsible for a measurable portion of the liquid transport and pressure drop. However, this comparison assumes that there is an equal rates of droplet entrainment and deposition within the control volume of the liquid film and there was no direct measure. Furthermore, while entrainment events, in the form of waves, were observed with the sensors, no droplet deposition events or impacts were observed.

Conclusions

Several studies have reported the pressure drop for microgravity two-phase flows. Unfortunately, most of these studies has been consisted of analyzing experimental by curve fitting or comparison against standard normal gravity models. Valid mechanistic models need to be developed and verified experimentally in order to ascertain the effects of fluid properties tube geometries and the acceleration so that system can be developed over a wide variety of applications, including those in a lunar, Martian, and normal gravity environments.

On the other hand, progress has been made with regards to prediction of pressure drop for bubble and slug flows, although there is still a significant amount of work required at low Re_L. The behavior of the liquid film in annular flow, in particular, the role of waves, and droplet entrainment and deposition needs to be further examined.

HEAT TRANSFER COEFFICIENTS

Determining the heat transfer coefficients is necessary to determine the size for heat exchangers. There are primary types of heat transfer coefficients: Condensation and evaporation heat transfer coefficients and boiling heat transfer coefficients. The difference between these type of heat transfer coefficients is the effect of the heat and mass tranfer on the thin liquid film. For the condensation and evaporation heat transfer coefficient, the heat is transferred through the flowing liquid film and the phase change occurs at the vapor liquid interface.

For the boiling heat transfer coefficient, the phase change occurs at the wall, and thus, the liquid layer adjacent to the solid heat transfer surface is perturbed by the nucleation and growth of a vapor region. This vapor region affects the distorts the flow within liquid layer since the liquid is a vapor source for the bubbles, condenses the vapor in the bubbles away from the heater surface, and also must either flow around the bubble or move it. Under certain situations, the vapor bubble may evolve into a large vapor film over the heater surface that has a much lower heat transfer coefficient than if liquid were present.

As such, the behavior of the liquid layer adjacent to wall or heat transfer surface becomes the focus of predicting the heat transfer coefficients. Previous studies in microgravity two-phase flow have shown the presence of a liquid film on the wall. Because of this, space system designers have focussed on dryout of that liquid film and eventual burnout of the tube wall being caused by excessive boiling or evaporation of the liquid film. As seen in Figure 7, this condition can also be obtained in microgravity because of the hydrodynamics. For some flow conditions in annular and slug flow, the liquid film slows and stops between the liquid slugs and roll waves. Actually, the liquid film is being stretched by the preceding slug or roll wave and then ruptures. Liquid is drained from the region by surface tension forces. Eventually, the area is rewetted by the next slug or roll wave. This periodic dryout can result in heating and quenching of localized areas of tube wall and eventually lead to failure of the tube wall.

Figure 7

One limitation to obtaining heat transfer coefficient data has been the difficulty of obtaining that data using ground-based, low-gravity facilities. For relatively slow flow rates, it may take a significant time for the flow regime to transverse the distance from its point of origin, either a mixer or boiler, to the instrumented portion of the test section. Then, additional time is required to effect a change in the thermal state of the heater and reach a new steady-state. This must be accomplished within 20 seconds.

A second problem that is encountered is the pooling and expulsion of vapor and liquid in various locations as the low-gravity experiment is transitioned from one acceleration level to another. Abdollahian *et al.* (1996) encountered this difficulty with their experiment within the boiling section. The flow direction was perpendicular to the direction of high-g acceleration encountered as the aircraft would begin its next trajectory. They suppositioned that the high-g's resulted in flow stratification, and the upper surface significantly warming as the liquid film drained from the surface, thus also reduced the amount of vapor generation. Upon entering the low gravity portion of the trajectory, there was a significant increase in the vapor generation rate and pressure, as this warm dry section was rewetted and more surface became available for boiling.

Nevertheless, data has been obtained for determining the two-phase heat transfer coefficients, both the condensation and evaporation heat transfer coefficients and the

boiling heat transfer coefficients.

Condensation and Evaporation Heat Transfer Coefficient

Hill and Best (1991) reported using a vapor-liquid system that condensation heat transfer coefficients for the same flowrates were less for microgravity conditions than normal gravity conditions. Their normal gravity data was obtained with their heat transfer sections being aligned horizontally, so as the liquid would condense on the top surfaces, the liquid would drain to the bottom, thus reducing the liquid film on the top surface and enhancing the heat transfer.

A series of studies have been conducted by Rite and Rezkallah (1993)[24], Rite and Rezkallah (1994)[25], Fore *et al.* (1996)[26], Rite and Rezkallah (1997)[27], and Fore *et al.* (1997)[28]. In these studies, they used air as the gas phase and a subcooled liquid, such as water. They rely on determining the heat transfer coefficient by sensibly heating the liquid phase. They found that the heat transfer coefficient in microgravity conditions was less than for similar flow conditions in vertical upflow or downflow in normal gravity. The Nusselt Number, *Nu*, and, thus, the heat transfer coefficient was determined empirically from experimental data as a function of a two-phase Reynolds Number, *Re*, and the liquid Prandtl Number, Pr_L.

In each study, they attributed the difference between the microgravity and normal conditions to the lack of buoyancy-driven shear between the gas phase and the liquid phase

resulting in very little mixing occuring within the phases. For bubble flow, this has been verified by the local velocity measurements made by Kamp *et al.* (1993)[29]. In both annular and slug flow, visual observations have confirmed that the liquid film on the wall will slow down, and sometimes stop, between the passage of liquid slugs and large disturbance waves. In vertical upflow, the liquid film is always moving. Until the shear forces of the phase in the core reach a sufficient level to overcome the buoyancy forces acting on the liquid film, the liquid film oscillates in its flow direction, up with the passage of large disturbances, such as slugs and large wave and down without these. This promotes mixing within the liquid layer adjacent to the wall.

Boiling Heat Transfer

Hill and Best (1991) reported a slight increase in the heat transfer coefficient between microgravity and normal gravity conditons. Abdollahian *et al.* (1996) reported only three data points for critical heat flux in a flow boiling system and did not draw any conclusions, but it is obviously from the data there were no order of magnitude differences betwen normal gravity and low gravity.

Westbye *et al.* (1995)[30] conducted boiling heat transfer tests that consisted of quenching a hot tube with subcooled Freon-113. As the liquid encountered the hot tube, it would vaporize. Experiments were conducted with the tube oriented horizontally in normal gravity and in reduced-gravity. Vapor film boiling heat transfer coefficients were higher in

microgravity than in normal gravity due to the thicker vapor film around the tube wall. However, when the boiling subsided, they found a decrease in the wall superheat for the boiling because of the higher heat transfer coefficient for the transition and nucleate boiling regimes.

Lee *et al.*[31] found similar increases in the boiling heat transfer coefficients in microgravity in a space-based experiment that also used Freon-113. This was for a pool boiling experiment and can be considered to a limiting case whereby the bulk liquid velocity approaches zero.

Conclusions

As was indicated earlier in the discussion of pressure drop, understanding the fundamental mechanisms is necessary in order to extend the predictive capability to other systems. This implies that the liquid layer at the wall and the relative mixing within the phases should receive attention.

NON-STRAIGHT FLOW CONDUIT

It is very possible that the majority of the pressure drop in space-based systems may occur within fittings as opposed to straight tubing. Although there may be some straight lengths of tubing that approach 1,000 L/D ratios in some space-based systems, a significant amount

of the total system pressure loss will occur within fittings. It is still worthwhile to study straight-tube pressure drop because of the uncertainty and because of the tendency to classify the pressure loss within a fitting as "equivalent pipe lengths."

McQuillen (1996)[32] examined visual data for both sudden expansions and contractions. Among the observations included the following:

• Sharp corners or edges can lead to dryout situations in the downstream portion of the fitting.

• Transition from the bubble to slug flow regime did not occur because of coalescence between radially-displaced bubbles, but from two other mechanisms. First, spherical bubbles with diameters greater than the contraction's diameter were squeezed into cylindrical bubbles. Second, If there were any bubbles that were immediately downstream of a cylindrical bubble as it entered the contraction, the trailing bubbles would catch up and coalescesce with the first bubble. This second effect has been seen in vertical up-flow in normal gravity and is attributed the lead cylindrical bubble having a much thinner liquid film around it which retards its motion in comparison to any trailing bubbles.

• For larger diameter ratio expansions, $D_{downstream}/D_{upstream}$, the existance of a two-phase jet was possible, as in Figure 8. This effect was not seen with smaller diameter ratios

Figure 8

Jayawardena and McQuillen (1996)[33] flowed air and various liquids through a 12.7 mm.

sidearm splitting tee and set flow resistances on the two exit legs at different values. A separation of the gas and liquid phases in one of the exit legs was accomplished via a free vortex separator that is describe by Shoemaker and Schrage (1997)[34], but there was still difficulty in obtaining a low gravity assessment of the liquid flowrate in the exit leg. Nevertheless, some important findings were made:

- The flow structures, such as slugs and waves, continued down the straight run with very little change in their spacing and velocity.
- Very little liquid flow down the sidearm branch came from the liquid film in the run of the tee, but from the liquid slugs and roll waves.
- There was a pressure recovery in both branches of the tee, similar to that of flow through an expansion.

Keshock and Lin[35] are planning to conduct tests with an air-water flow through a helicoil length of tubing to ascertain the effect that the centrifugal action will place on the flow.

While the amount of research that has been conducted in this area is very limited, there are plans to continue and expand this line of research.

VOID FRACTION AND FILM THICKNESS

Several authors have published data concerning either void fraction, or average gas velocity, and film thickness. In the studies of Colin *et al.* (1991), Colin and Fabre (1995),

Bousman and Dukler (1993), Bousman (1995), conductance probes were used to determine the cross-sectional averaged void fraction α. The cross-sectional averaged gas velocity, U_G, was determined from flow visualization (Colin and Fabre, 1995) or by cross-correlating the signals from two pairs of wire probes positioned along the tube axis (Bousman and Dukler, 1993). The measured values of gas velocities, U_G, compare well to those calculated from the experimental void fraction (Colin and Fabre, 1995) $U_G = j_G/\alpha$ and the gas velocity is reasonably well predicted by the classical drift flux models (Zuber and Findlay, 1965[36]):

$$U_G = C_0(j_G + j_L),\ 1.1 < C_0 < 1.3 \qquad (8)$$

In bubbly and slug flow in microgravity, the gas velocity is always greater than the liquid velocity, even in the absence of a driving force. Where does the drift come from in the absence of gravity?

Local measurements carried out by Kamp (1996)[37] in bubbly flow proved that the local drift between phases is negligible. The local liquid velocity, measured with a hot wire probe, is nearly the same as the local bubble velocity, measured with a double optical probe, as seen in Figure 9. However, the gas is mainly concentrated in the flow regions where the velocity is the greatest, i.e. at the tube axis (Figure 10). From the radial profiles of void fraction and velocities and following Zuber and Findlay (1965), it is possible to calculate the value of C_0. The values are in good agreement with those obtained with the conductance probes.

Figures 9 & 10

The effect of spatial distribution demonstrates that there is an average drift in bubbly flow even if there is no local slip. Therefore, the key issue for bubbly flow is to determine why the bubbles are concentrated near the axis. The answer to this question requires local measurements of void fraction, liquid and gas velocities.

As was previously mentioned, C_0 can be calculated for slug flow using the same methods for bubbly flow. This was pointed out by Colin *et al.* (1991) based on their experiments in a 40 mm diameter tube and was also confirmed by the experiments in smaller tubes and by Bousman and Dukler (1993). In slug flow, the gas is mostly contained in the large cylindrical bubbles. Thus, it is acceptable to assume that $U_G \approx V$, where V is the velocity of the cylindrical bubbles. The results show that the Nicklin *et al.* (1962)[38] relationship for turbulent flow $V = 1.2(j_L + j_G) + 0.35(gD)^{1/2}$ is valid also for C_0 at the limit of $g \to 0$. From the inviscid flow theory of Collins *et al.* (1978)[39], C_0 is highly sensitive to the flow regime upstream of the cylindrical bubbles as in the following equation:

$$C_o = 2.27 \quad \textit{for laminar flow}$$
$$C_o = \frac{\log(Re_L) + 0.089}{\log(Re_L) - 0.74} \quad \textit{for turbulent flow} \qquad (17)$$

In particular, its value is predicted to increase from 1.2 to 2.27 when the flow becomes laminar. In normal gravity flow, this behavior was clearly shown by Fréchou (Fabre and Liné[40], 1992).

Some additional experiments are thus necessary to determine the behavior of C_0 for Re_L within the range 500–5,000. Indeed in this range, the laminar to turbulent transition —which must exist— is highly indicative of a modification of flow regime upstream the nose of the cylindrical bubble. An indication of the turbulence level could be obtained from a wall shear stress probe as was used by Bousman and McQuillen (1994) for annular flows.

The repartition of the phases between the cylindrical bubbles and the liquid slugs is also of interest for slug flow and has not yet received a definitive answer so specific experiments need to be carried out. One question is whether the rate of occurrence of the long bubbles is dependent upon the entrance conditions at the mixer or not.

As was stated earlier, the liquid film and its interaction with the gas core in annular flow are significant with respect to both the pressure drop and heat transfer coefficients. Bousman (1995) measured film thickness using conductivity probes and cross-correlating signals to obtain velocities. Bousman and McQuillen (1994) found with five sets of probes placed at 90° intervals around the circumference of the tube and 1 cm intervals axially. They found that for conditions aboard the aircraft during the low-gravity trajectory, not only was the substrate for the annular film symmetrical around the tube circumference, so were the large

disturbance or roll waves. They also showed that high liquid velocities increased the average film thickness and high gas velocities decreased the thickness.

The effect of surface tension and liquid viscosity wee examined by Bousman and McQuillen (1994) through the use of water, a 50% water and glycerine mixture, and a water and surfactant mixture. The water and glycerine solution had the largest waves and liquid film thickness while the water and surfactant mixture had the least. They theorized that a reduction in surface tension and viscosity increased the droplet atomization from waves, thus transferring the amount of liquid being carried from the liquid film and waves to the gas core.

Bousman (1995) found that the liquid wave was more symmetrical about itself in the flow direction in microgravity than in a falling film in normal gravity. He also compared the microgravity data against relationships for liquid film thickness developed by Kosky(1971)[41] and Henstock and Hanratty(1976)[42] and had mixed results. Bousman (1995) empirically determined the following relationship.

$$h_L^+ = \frac{h\left(\tau_w / \rho_l\right)^{1/2}}{\nu_L} = 0.265\, Re_L^{0.695} \qquad (18)$$

where h_L^+ is a dimensionless film thickness and h is the actual film thickness.

Conclusions

Void fraction and liquid film thickness measurement are possible by using several different techniques. As was pointed out earlier, careful measurement of these quantities are necessary to develop mechanistic models for the pressure drop and heat transfer coefficients. Unfortunately, the literature only consists of measurements that have been made for air-water and water mixtures. There is no reported data for refrigerant or other fluid systems in a microgravity environment.

LOCAL CHARACTERISTICS OF BUBBLY FLOW

The understanding of the dynamics of two-phase flows at microgravity requires an analysis of the local flows. The local structure of a bubbly pipe flow has been experimentally and theoretically investigated by Kamp (1996). This study examined two mains problems of bubble flow: The evolution of the bubble size along the pipe length due to coalescence, and the radial distribution of bubbles in the pipe. The repartition and the morphology of the bubbles control the momentum and heat transfer at the wall and between the phases.

Kamp (1996) developed a criterion to determine the maximum bubble size that could be examined based on the acceleration levels by calculating the effect of a typical trajectory that can be classified as "bumpy" on the motion of a single 1 mm diameter bubble in a stagnant liquid. He determined that the drag (FD) and buoyancy forces (FA) played a greater influence on the bubble trajectory than the history (FH) and added mass (FMA) forces as shown in Figure 11. The added mass forces are those associated with the using

approximations to compensate for two bubbles of different sizes that may coalesce. By assuming that the residual gravity level should be approximated by a sinusoidal function of amplitude g_0 and pulsation ω_0, the equation governing the motion of one bubble can be written by neglecting history and added mass forces :

$$6\pi\mu_L dv = \frac{\pi d^3}{6} g_0 \sin(\omega_0 t) \tag{19}$$

After integrating Equation 19, the radial displacement z of the bubble is obtained and must be very small compared to the pipe diameter D:

$$\frac{z}{D} = \frac{d^2 g_0}{36\omega_0 \nu_L D} << 1 \tag{20}$$

He concluded that for $g_0 = 0.2$ m/s and $\omega_0 = 2\pi 0.3$ rad/s, d^2 / D has to be smaller than $3\text{x}10^{-4}$ m. Thus, in order to minimize the effect of typical aircraft acceleration transients on radial bubble motion, the bubble diameter could not be larger than 3 mm.

Bubble Coalescence

An approximate model for bubble coalescence in a turbulent pipe flow under microgravity conditions has been developed by Kamp(1996) and Kamp *et al.*(1996)[43] Because of the absence of mean relative bubble velocity with the liquid phase, as was illustrated in Figure 9, the collisions are purely turbulence-induced and the collision rate can be estimated by statistical considerations. A coalescence probability is derived from the ratio of the film

drainage time between approaching bubbles and the interaction time during bubble collisions. The transport equations for the interfacial area density and specific diameter are numerically solved with a one-dimensional approximation to yield the bubble size evolution along the pipe. The results show good agreement with previously obtained data (Colin, 1990[44]). From the bubbly flow pictures, the probability density functions (pdf) of bubble diameters are determined, using image processing, at the inlet and outlet (80*D* downstream) sections of the tube. The pdf of the bubble diameters (d) are well fitted by a log-normal law (Kamp, 1996). The log-normal distribution is defined by two parameters: a characteristic d_{00} and a parameter indicating the width $\hat{\sigma}$:

$$P(d) = \frac{1}{d\sqrt{2\pi\hat{\sigma}^2}} \exp\left[-\frac{(\mathrm{Ln}(d/d_{00}))^2}{2\hat{\sigma}^2}\right] \qquad (13)$$

The predicted values of the d_{00}, $\hat{\sigma}$, as well as the Sauter mean diameters are plotted versus the measured values in Figure 12. Good agreement is achieved, except for the large bubble diameters (case E07, D03), where the model is no longer valid.

After validation of the model by comparison with experimental data, it was used to predict the influence of the gas fraction, the bubble diameter at the pipe inlet and the liquid superficial velocity j_L on the coalescence rate. Simulations were performed for the following range of the parameters: $0.2 \text{ m/s} < j_L < 2 \text{ m/s}$, $0 < \bar{\alpha} < 0.15$, $0.5 \text{ mm} < d_{00} < 4 \text{ mm}$ and $\hat{\sigma} = 0.25$. The main results of the simulations are summarized as follows:

- The coalescence rate proves to be approximately proportional to the void fraction.
- The residence time in the tube is an important parameter that must be taken into account in the comparison of data at different liquid flow rates.
- At constant residence times, the coalescence rate increases as the turbulence intensity increases due to an increase in collision rate.
- The bubble diameter at the inlet of the pipe is an important parameter for the evolution of the bubble size along the pipe. Since this effect is non-linear, the ratio between the bubble size and bubble size at the inlet is not a pertinent parameter.
- The coalescence rate is very high for small bubbles, but gradually decreases along the pipe due to an increase in the bubble Weber number. This means that it might be possible to reach a steady state where the Weber number is of order 1 and no more collision takes place, at least if the transition to slug flow has not appeared yet.

The coalescence rate in microgravity turbulent pipe flow is correctly predicted when the bubble size remains smaller than the integral length scale of turbulence (D/4) and when the collision between bubbles are only turbulence-induced. This model is not yet able to predict the coalescence rate in small tube experiments. It should be extended to the prediction of the coalescence rate for larger bubbles in order to reach the transition to slug flow and should also take into account the collision between bubbles induced by the mean velocity gradient.

Radial Void Fraction Distribution

The first local measurements in bubbly flow in microgravity have been carried out by Kamp *et al.* (1993) and compared to vertical up-flow and downflow. For a relevant comparison of the results, the bubble size had to be the same in the normal gravity and reduced-gravity experiments, so coalescence in microgravity was inhibited by adding a small amount of surfactant (Sodium Dodecyle Sulfate). Moreover, by reducing bubble size in microgravity, the influence of the residual buoyancy force compared to other surface forces is also reduced. Void fraction, bubble velocity and bubble size were measured by a double optical fiber probe and the velocity of the liquid phase by hot film anemometry. For bubbly flow, the radial void profile would peak near the center for reduced-gravity and normal gravity downflow; however, for normal gravity vertical up-flow, the void would peak near the walls (Figure 10). The local measurement of liquid and gas velocity confirm the near zero value of the drift velocity reduced-gravity conditions (Figure 9).

In normal gravity experiments, the void fraction distribution is mainly controlled by the lift force inducing void coring effect in downward flow and wall peaking in upward flow. The void coring in reduced-gravity is not clearly explained at the present time, and the local two-fluid models fail to predict the correct distribution. Until recently, classical two-fluid models were unable to predict correct void fraction distribution in microgravity flows. In the

absence of drift velocity, the drag and lift forces acting on the bubbles disappear. Then the motion of the bubbles is controlled by the added mass and Tchen forces. The void coring effect should be attributed to the turbulence of the liquid phase through these forces acting on the bubbles.

Conclusions

Tracking the motion of a single bubble in a pipe at microgravity conditions, either experimentally or numerically, would be helpful to understand the void coring effect. On the other hand, the experimental analysis of the local distributions of velocity and void are also of great help.

The techniques to measure liquid droplet velocity and size distribtuions in annular flow has been developed in normal gravity, but these techniques now need to be conducted in microgravity in order to study droplet dynamics during the entrainment and deposition process.

CONCLUSION

During the past decade, a considerable effort has been done to understand two-phase flow at microgravity conditions. Spacecraft system designers need data regarding the pressure drop, heat transfer coefficients and system stability. As a result, several studies have been

conducted concerning flow pattern transitions and, pressure drop and heat transfer coefficients.

While there has been a significant amount of work that has been undertaken, the development of mechanistic models has been limited thus limiting the extension of this data to other applications that could include differences in fluid properties, tube geometry and acceleration levels. The development of mechanistic models and the use of the microgravity environment as a research tool can be used to effectively develop a better understanding of the behavior of gas-liquid flows in normal gravity as well.

In particular, models need to be developed that address the effect of gravity, from vertical up-flow through microgravity to vertical down-flow, on turbulence for bubble flow, the flow within the liquid film in both slug and annular flow, the flow within liquid slugs, the structure of waves and their role in droplet formation, and the behavior of droplets in annular flow.

Local measurements of phase velocities and voids, slug and roll wave velocities, void and film thickness are required in order to develop these models.

---

[1] T. Swanson, A. Juhasz, W. R. Long, and L. Ottenstein, "Workshop on Two-Phase Fluid Behavior in a Space Environment," *NASA Conference Publication 3043* (1989).

[2] D. Barnea, "A Unified Model for Predicting Flow-Pattern Transitions for the Whole

Range of Pipe Inclinations," *International Journal of Multiphase Flow,* **13**, 1-12 (1987).

[3] D. G. Evans, "Visual Study of Swirling and Nonswirling Two-Phase Two Component Flow at 1 and 0 Gravity," *NASA Technical Memorandum X-725* (1963).

[4] J. A. Albers, and R. P. Macosko, "Experimental Pressure Drop Investigation of Non-Wetting Condensing Flow of Mercury Vapor in a Constant Diameter Tube in 1 G and Zero Gravity," *NASA Technical Note D-2838* (1965).

[5] D. B. Heppner, J. C. King, and J. W. Littles, "Zero G Experiments in Two-phase Fluid Flow Regimes," *ASME Paper 75-ENAS-24* (1975).

[6] D. B. Heppner, J. C. King, and J. W. Littles, "Aircraft Flight Testing of Fluids in Zero Gravity Experiments," *General Dynamics Report CASD NAS-74-054* (1978).

[7] C. Colin, J. Fabre, and A. E. Dukler, "Gas Liquid Flow at Microgravity Conditions I. Dispersed Bubble and Slug Flow," *International Journal of Multiphase Flow,* **17**, 533-544 (1991).

[8] A. E. Dukler, J. A. Fabre, J. B. McQuillen, and R. W. Vernon, "Gas-Liquid Flow at Microgravity Conditions: Flow Patterns and Their Transitions," *International Journal of Multiphase Flow,* **14**, 389-400 (1988).

[9] L. Zhao, and K. S. Rezkallah, "Gas-Liquid Flow Patterns at Microgravity Conditions," *International Journal of Multiphase Flow,* **19**, 751-763 (1993).

[10]C. Colin, J. Fabre, "Gas-Liquid Pipe Flow Under Microgravity Conditions: Influence Of Tube Diameter On Flow Patterns And Pressure Drops," *Adv Space Res,* **16**, 137-142,

(1995).

[11]C. S. Huckerby, and K. S. Rezkallah, "Flow Pattern Observations in Two-phase Gas Liquid Flow in a Straight Tube under Normal and Microgravity Conditions," *Proceedings of the National Heat Transfer Conference,* San Diego, CA July 1992, American Institute of Chemical Engineers (1992).

[12]W. S. Bousman, and A. E. Dukler, "Ground Based Studies of Gas-Liquid Flows in Microgravity Using Learjet Trajectories," *AIAA 94-0829* (1994).

[13]W. S. Bousman, "Studies of Two-Phase Gas-Liquid Flow in Microgravity", *NASA Contractor Report 195434* (1995).

[14]C. Colin, J. Fabre, J. McQuillen, "Bubble and slug flow at microgravity conditions:state of knowledge and open questions," *Chem. Eng. Comm,* **141-142,** 155-173 (1996).

[15]W. S. Hill, and F. R. Best, "Microgravity Two-Phase Flow Experiment and Test Results," *SAE Technical Paper Series 911556* (1991).

[16]W. S. Bousman, and J. B. McQuillen, "Characterization of Annular Two-Phase Gas-Liquid Flows in Microgravity," *NASA Conference Publication 3276* (1994).

[17]S. Jayawardena, V. Balakataiah, and L. C. Witte, "Flow Pattern Transition Maps for Microgravity Two-Phase Flows, *AIChE Journal,* **43,** 1637-1640 (1997).

[18]I.Y. Chen, R. S. Downing, E. Keshock and M. Al-Sharif, "Measurements and Correlation of Two-Phase Pressure Drop Under Microgravity Conditions," *Journal of Thermophysics and Heat Transfer,* **5,** 514-523 (1991).

[19]G. B. Wallis, *One-Dimensional Two-Phase Flow,* New York, McGraw-Hill (1969).

[20]A. E. Dukler, and J. A. Fabre, "Gas-Liquid Slug Flow: Knots and Loose Ends," *Third International Workshop on Two-Phase Flow Fundamentals*, London, UK, June 15-19, 1992.

[21]L. Zhao and K. S. Rezkallah, "Pressure Drop in Two-Phase Annular Flow at Microgravity Conditions," *AIAA 93-0572* (1993).

[22]D. Abdollahian, J. Quintal, F. Barez, J. Zahm and V. Lohr "Study of Critical Heat Flux and Two-Phase Pressure Drop Under Reduced-gravity," *NASA Contractor Report 198516* (1996).

[23]L. Zhao and K. S. Rezkallah, "Pressure Drop in Gas-Liquid Flow at Microgravity Conditions," *Int. J. Multiphase Flow*, **21**, 836-849 (1995).

[24]R. W. Rite and K. S. Rezkallah, "An Investigation of Transient Effects on Heat Transfer Measurements in Two-Phase, Gas-Liquid Flows Under Microgravity Conditions," *HTD-Vol. 235, Heat Transfer in Microgravity Systems,* ASME (1993)

[25]R. W. Rite and K. S. Rezkallah, "Heat Transfer in Two-Phase Flow Through a Circular Tube at Reduced-gravity," *Journal of Thermophysics and Heat Transfer,* **8**, 702-708 (1994).

[26]L. B. Fore, L. C. Witte, and J. B. McQuillen, "Heat Transfer to Annular Gas-Liquid Mixtures at Reduced-gravity," *Journal of Thermophysics and Heat Transfer,* **10**, 633-639 (1996).

[27]R. W. Rite and K. S. Rezkallah, "Local and Mean Heat Transfer Coefficients in Bubbly and Slug Flow Under Microgravity Conditions," *Int. J. Multiphase Flow,* **23**, 37-54

(1997).

[28]L. B. Fore, L. C. Witte, and J. B. McQuillen, "Heat Transfer to Two-Phase Slug Flows Under Reduced-Gravity Conditions," *Int. J. Multiphase Flow*, **23**, 301-311 (1997).

[29]A. Kamp, C. Colin, J. Fabre, "Bubbly Flow In A Pipe: Influence Of Gravity Upon Void And Velocity Distributions", *Proceeding of the 3rd World Conference on Experimental Heat Transfer, Fluid Mechanics and Thermodynamics*, Honolulu, USA, 1418-1424 (1993).

[30]C. J. Westbye, M. Kawaji, and B. N. Antar, "Boiling Heat Transfer in the Quenching of a Hot Tube Under Microgravity," *Journal of Thermophysics and Heat Transfer*, **9**, 302-307 (1995).

[31]H. S. Lee, H. Merte, Jr., and F. Chiaramonte, "Pool Boiling Curve in Microgravity," *Journal of Thermophysics and Heat Transfer*, **11**, 216-222 (1997).

[32]J. McQuillen, "Observations of Gas-Liquid Flows Through Contractions in Microgravity," *NASA Conference Publication 3338*, pp. 95-102 (1996).

[33]S. Jayawardena and J. McQuillen, "Microgravity Two-Phase Flow at a Pipe Junction," *AIAA 96-2070* (1996).

[34]J. M. Shoemaker and D. S. Schrage, "Microgravity Fluid Separation Physics: Experimental and Analytical Results," *AIAA 97-0886* (1997).

[35]E. G. Keshock and C. S. Lin, "Two-Phase Annular Flow in Helical Coil Flow Channels in a Reduced-gravity Environment," *NASA Conference Publication 3338* (1996).

[36]N. Zuber, J. A. Findlay, "Average volumetric concentration in two-phase flow systems,"

J. Heat Transfer, **87**, 453–68 (1965)

[37]A. Kamp, "Ecoulements turbulents à bulles dans une conduite en micropesanteur", Thesis of Institut National Polytechnique of Toulouse, France (1996).

[38]D. J. Nicklin, J. O. Wilkes, J. F., Davidson, "Two-phase Flow in Vertical Tubes," *Trans. Inst. Chem. Engs.*, **40**, 61-68 (1962).

[39]R. Collins, F. F. de Moraes, J. F. Davidson, D. Harrison, "The Motion of Large Bubbles Rising Through Liquid Flowing in a Tube," *J. Fluid Mech.*, **89**, 497–514 (1978).

[40]J. Fabre, A. Liné, "Modelling of Two-phase Slug Flow," *Annu. Rev. Fluid Mech.*, **24**, 21-46 (1992).

[41]P. G. Kosky, "Thin Liquid Films Under Simultaneous Shear and Gravity Forces," *Int. J. Heat Mass Transfer*, **14**, 1220-1224, 1971.

[42]W. H. Henstock and T. J. Hanratty, "The Interfacial Drag and the Height of the Wall Layer in Annular Flows," *AIChE J.*, **22**, 990-1000, 1976.

[43]A. Kamp, C. Colin, J. Fabre , "Prediction of bubble sizes in microgravity gas-liquid pipe flows," 2nd Symposium on Fluids in Space, Naples, Italy, April 22-26th, 1996.

[44]C. Colin, " Ecoulements diphasiques à bulles et à poches en micropesanteur", thèse de l'Institut National Polytechnique de Toulouse, France (1990).

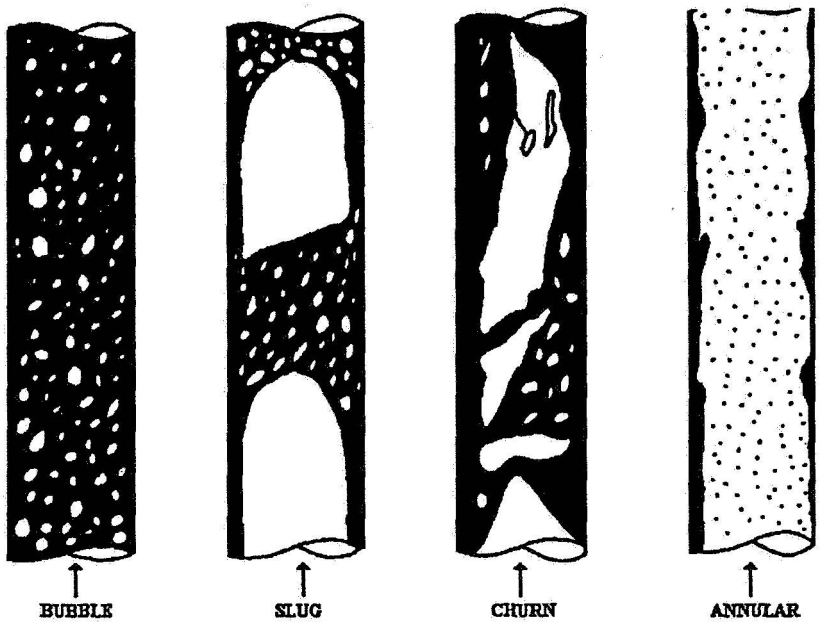

Figure 1: Normal Gravity Vertical UpFlow Regimes

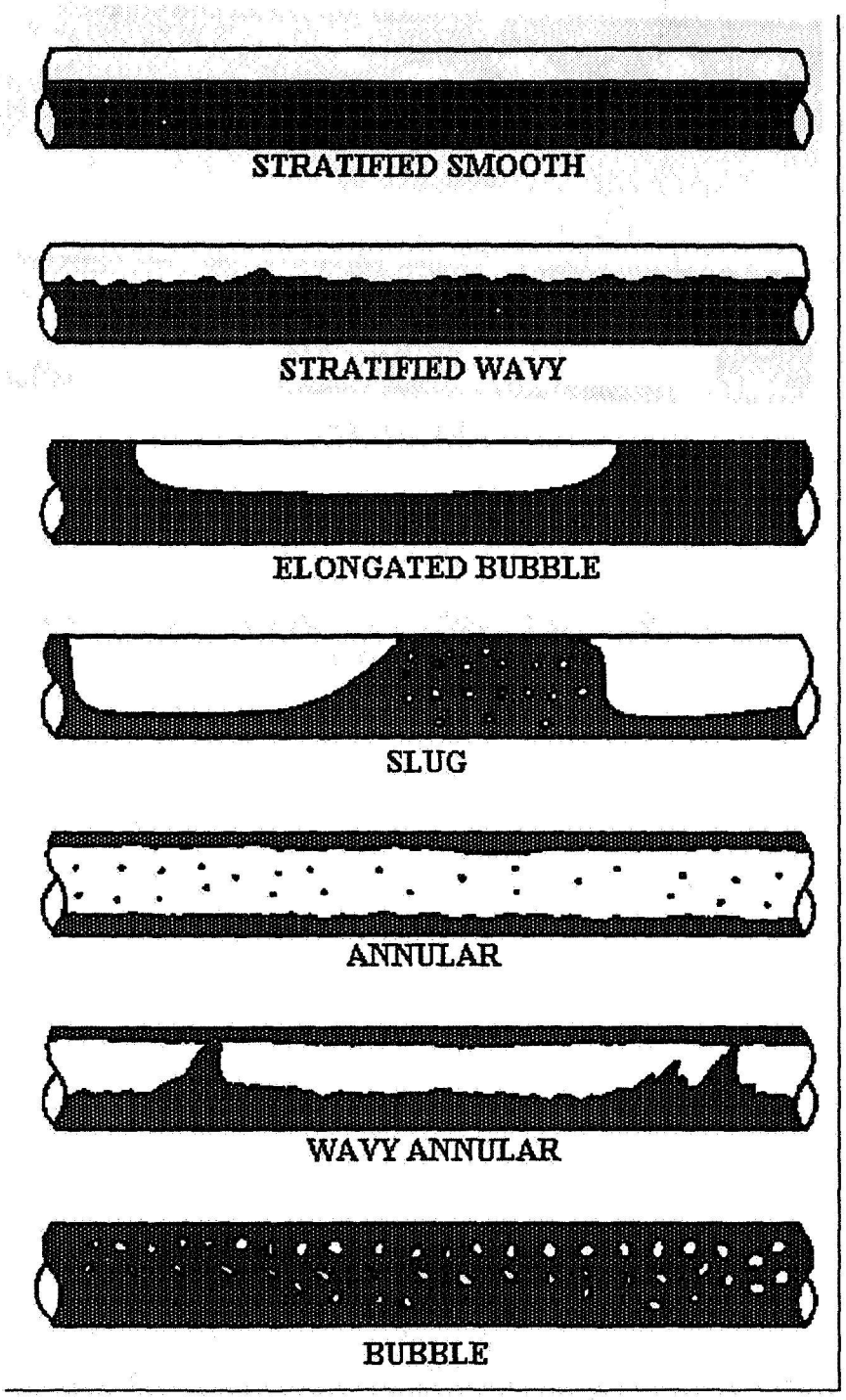

Figure 2: Normal Gravity Horizontal Flow Regimes

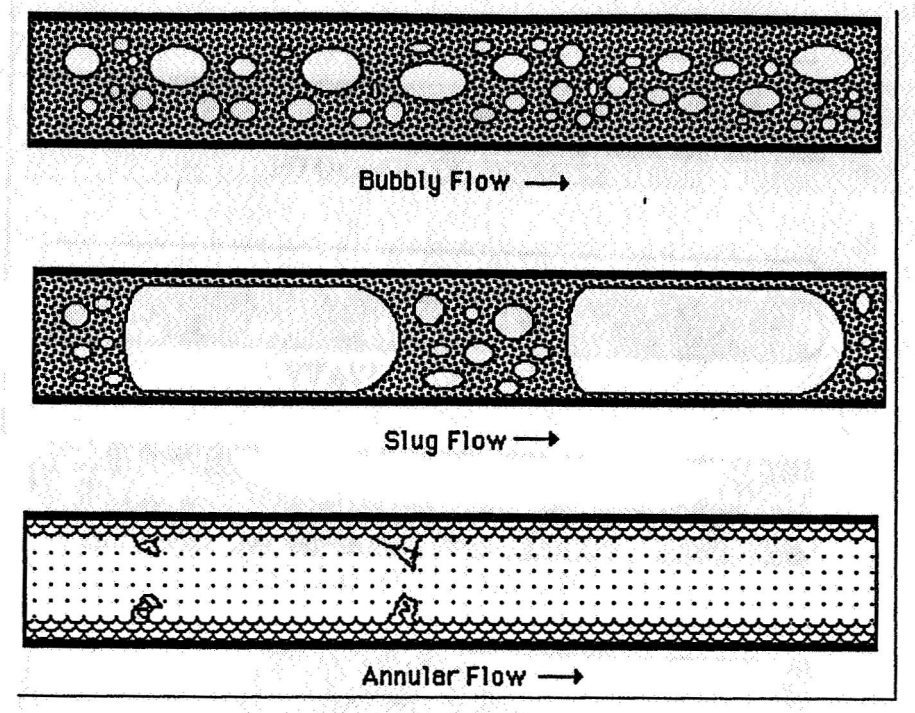

Figure 3: Reduced Gravity Flow Regimes

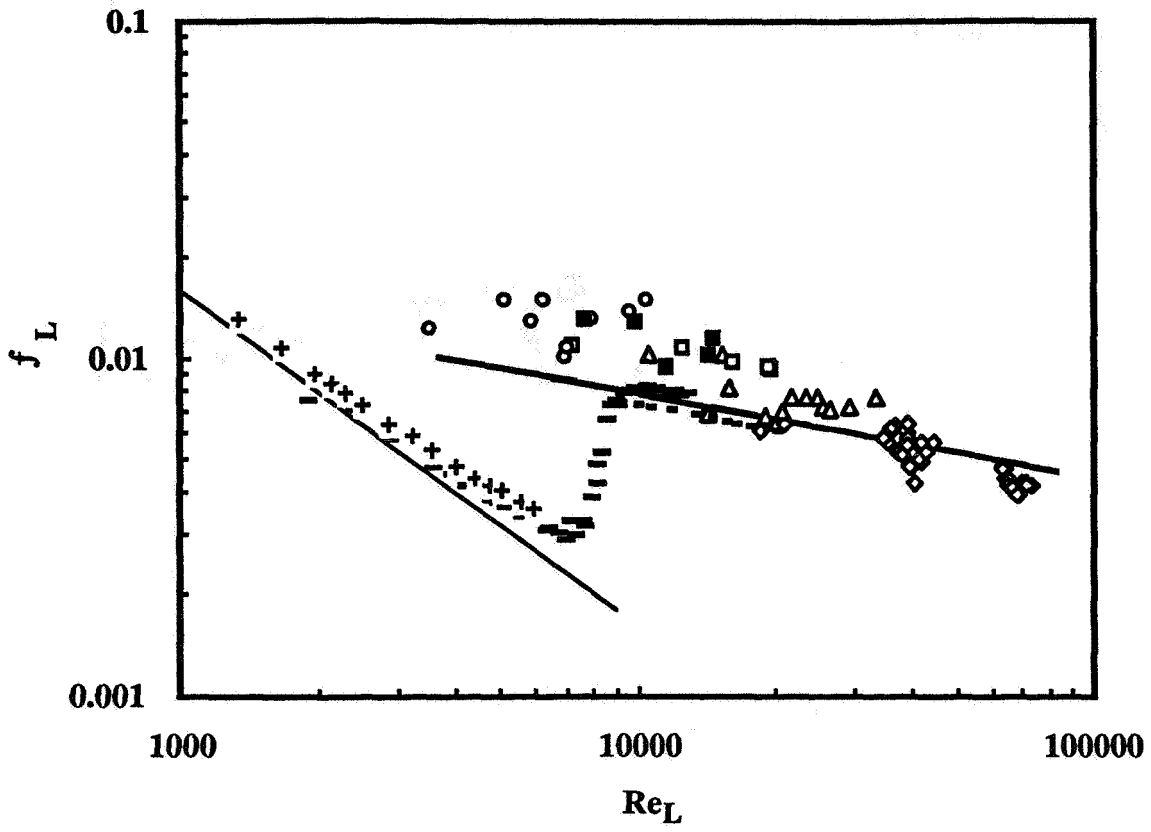

Figure 4: Wall Friction Factors f_L in Bubbly Flow (Colin, *et al.*, 1996)

0-g flow ○ D=6 mm, □ D=10 mm, △ D=19 mm, ■ D=12.7 mm, ◇ D=40 mm

single-phase flow: + D=6 mm – D:10 mm - D=19 mm

Blasius, —— Poiseuille relationship

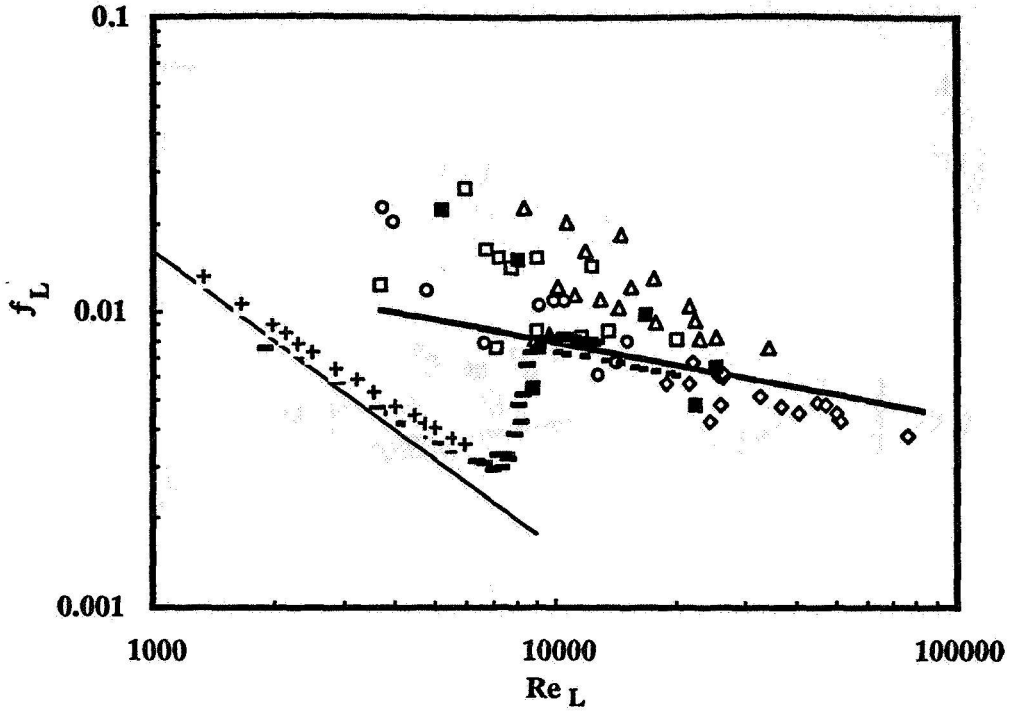

Figure 5: Wall Friction Factors f_L in Slug Flow (Colin, *et al.*, 1996)

0–g flow ○ D=6 mm, □ D=10 mm, △ D=19 mm, ■ D=12.7 mm, ◇ D=40 mm

single-phase flow: + D=6 mm – D:10 mm - D=19 mm

Blasius, —— Poiseuille relationship

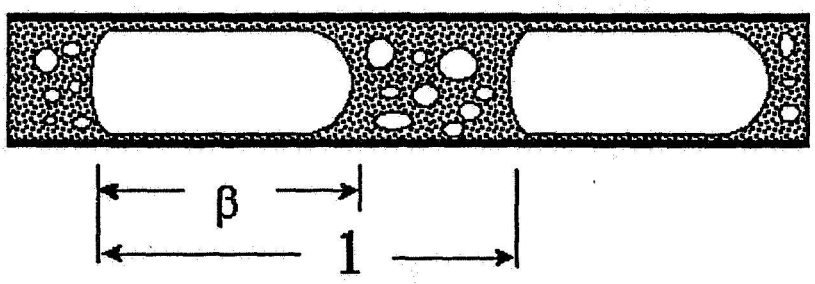

Figure 6: Unit Cell Concept for Slug Flow

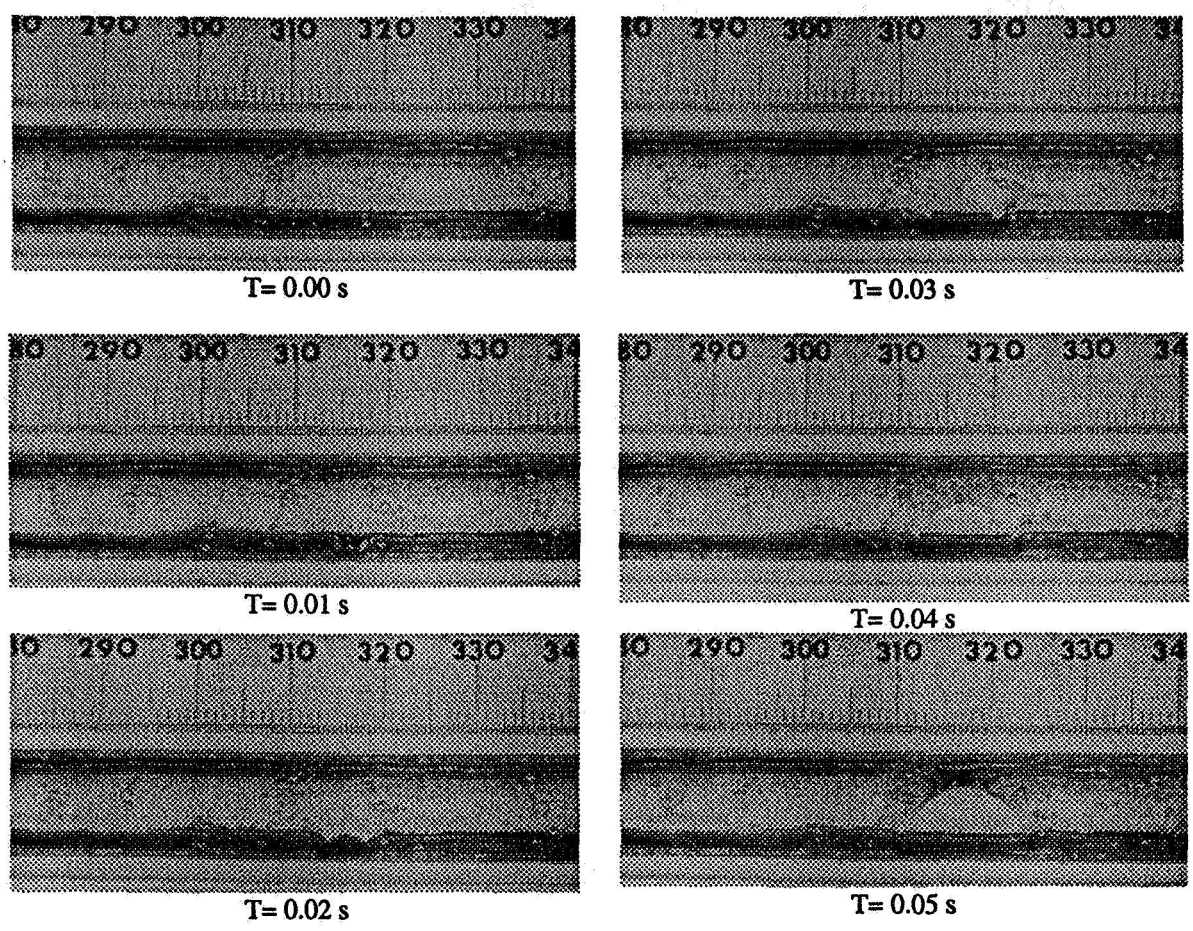

Figure 7: Liquid Film Rupture and Drainage in Microgravity at x = 315 Marker

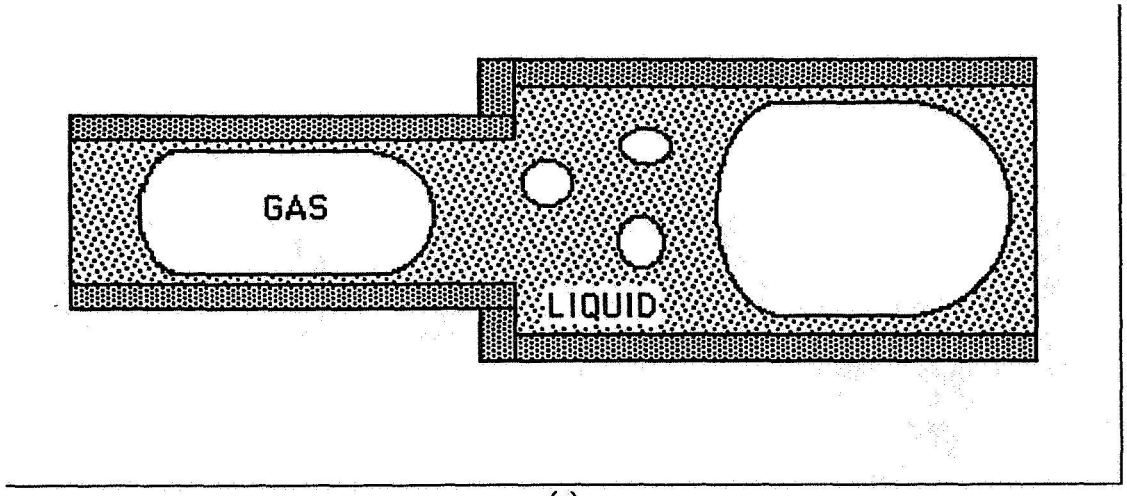

(a)

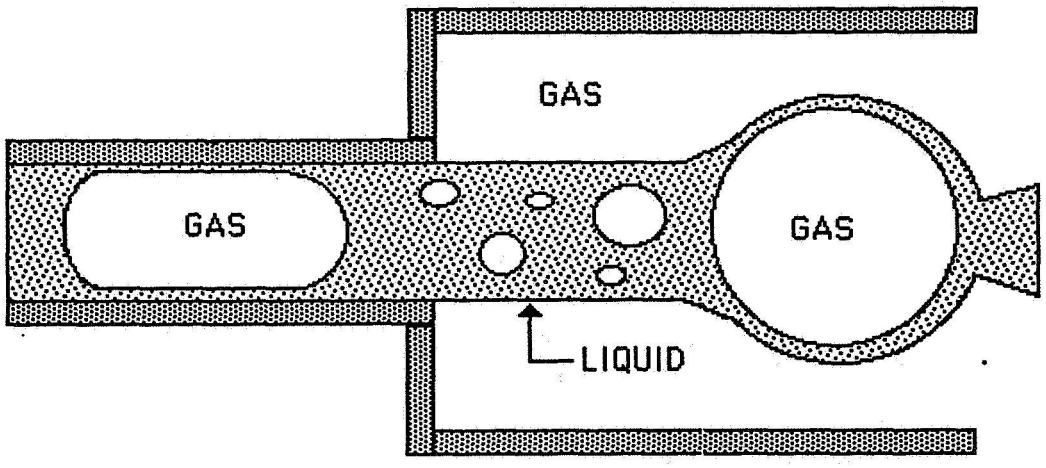

(b)

Figure 8: Flow through a sudden expansion

a - 3/4 diameter ratio, b- 3/8 diameter ratio

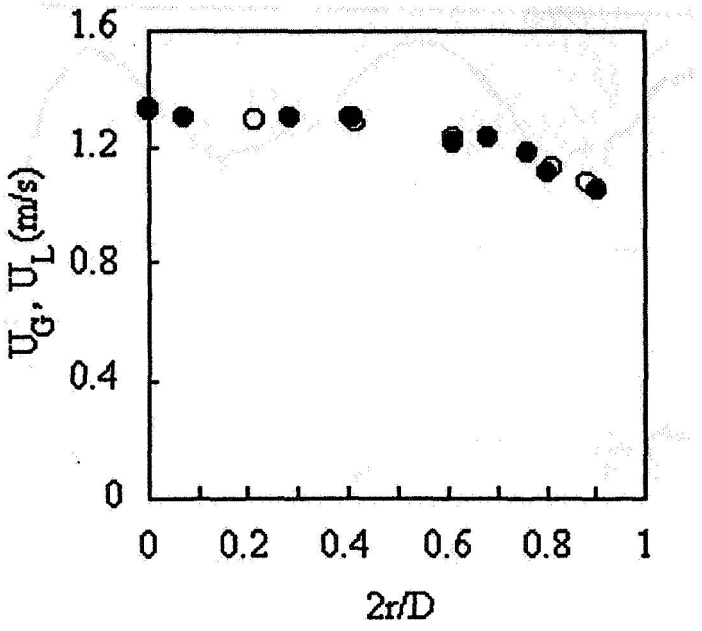

Figure 9: Gas and Liquid Velocity Distribution in Microgravity (Kamp, 1996)

open symbol - gas and dark symbols - liquid

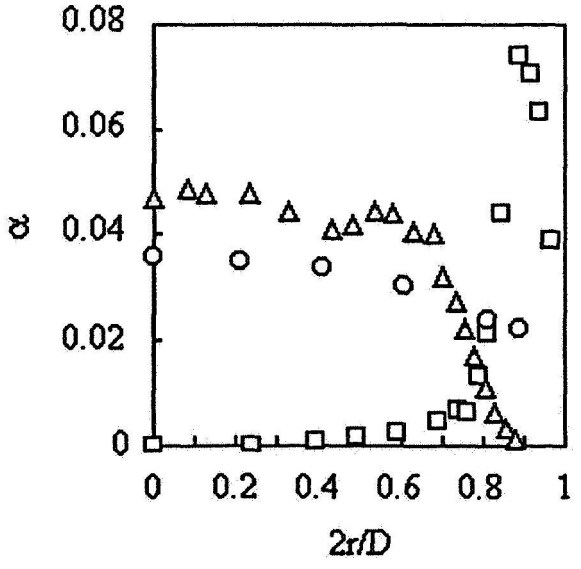

Figure 10: Radial Void Fraction Distributions (Kamp, 1996)

□ Upward, △ Downward, o Microgravity

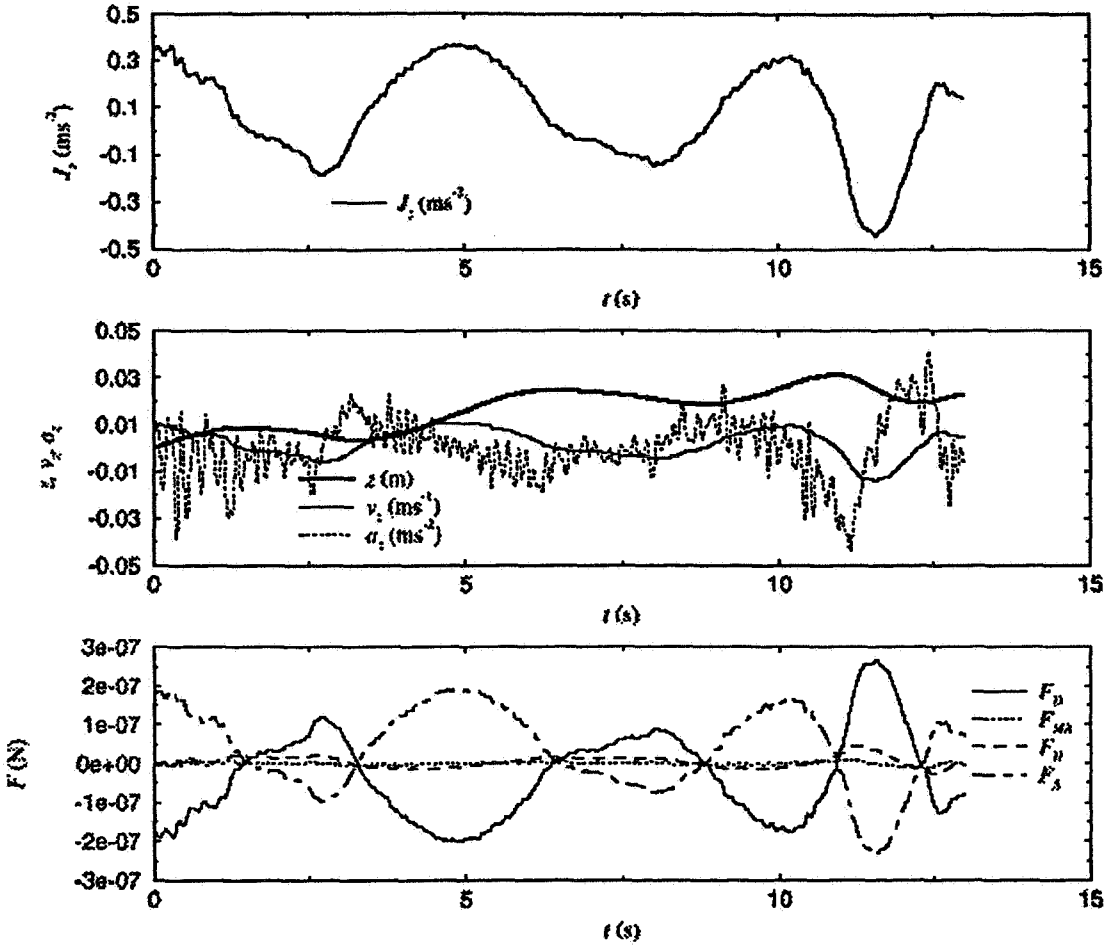

Figure 11: Acceleration Levels and Forces Acting on a Bubble During a Typical Trajectory (Kamp, 1996)

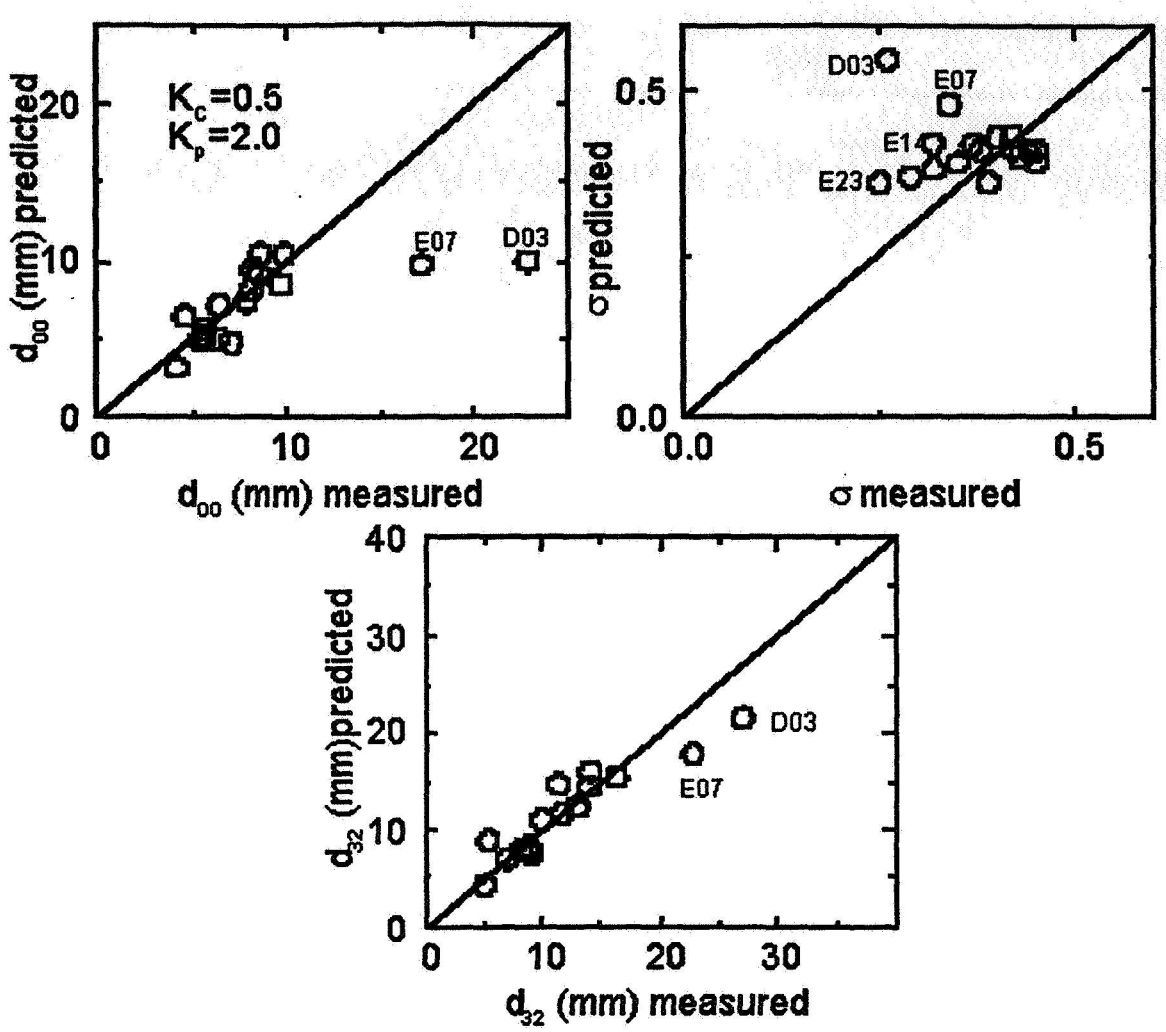

Figure 12: Measured and Predicted Medians, Distribution Widths and Sauter Diameters (Kamp, 1996)